Valorization of handmade argan press cake by supercritical CO2 extraction

Adil Mouahid, Magalie Claeys-Bruno, Isabelle Bombarda, Sandrine Amat, Andrea Ciavarella, Emmanuelle Myotte, Jean-Paul Nisteron, Christelle Crampon, Elisabeth Badens

Valorization of handmade argan press cake by supercritical CO_2 extraction

Adil Mouahid[a,*], *Magalie Claeys-Bruno*[b], *Isabelle Bombarda*[b], *Sandrine Amat*[b], *Andrea Ciavarella*[a], *Emmanuelle Myotte*[a], *Jean-Paul Nisteron*[a], *Christelle Crampon*[a], *Elisabeth Badens*[a]

[a] *Aix Marseille Univ, CNRS, Centrale Marseille, M2P2, Marseille, France*
[b] *Aix Marseille Univ, Avignon Université, CNRS, IRD, IMBE, Marseille, France*

ARTICLE INFO

Article history:
Received 19 August 2022
Received in revised form
18 November 2022
Accepted 28 November 2022
Available online 2 December 2022

Keywords:
Handmade Argan press cake
Supercritical CO_2 extraction
Valorization
Edible oil

ABSTRACT

The capability of supercritical CO_2 to extract edible oil from handmade Argan press cake was investigated. The aim is to enable Moroccan cooperatives to improve their economic situation by valuing the handmade argan press cake, which is nowadays considered as a waste, applying a clean extraction process. Extraction experiments were conducted at 300 and 400 bar, 333 K and 0.14 kg/h on dried biomass. The fatty acids and tocopherols compositions of the extracted oil were found similar to previous studies and correspond to a commercial edible oil. The air flow dried biomass exhibits a higher extraction yield compared to the freeze-dried biomass. A pressure of 300 bar seems to be sufficient to allow the extraction of oil with a satisfactory extraction kinetic.

1. Introduction

The Argan kernel can contain up to 63% of oil (Mouahid et al., 2022, 2021) and the benefits of argan oil have already been demonstrated: antioxidant, healing properties, ω-3 and ω-6 fatty acid content, etc. Argan oil is therefore very well known for its application in food, cosmetics and pharmaceutical industries. Edible oil is obtained from roasted kernels while cosmetic oil is produced from unroasted kernels. Argan oil can be handmade or obtained using an industrial scale mechanical process (Charrouf and Guillaume, 2008). The production of edible handmade Argan oil is basically performed in artisanal cooperatives which aim to improve the socio-economic conditions of rural women in Morocco. The edible handmade argan oil is then produced by Berber women following a traditional process: argan kernels are roasted in a pan or in a clay plate for few minutes, the roasted kernels are then crushed in an artisanal millstone (Azerg in Berber) leading to the formation of a brown viscous dough. The dough is then hand kneaded with the addition of tepid water leading to the formation of an emulsion. Argan oil is obtained after the settling (about two weeks) of the emulsion with an extraction yield (mass of oil reported to the mass of biomass) ranging from 25% to 30%, which is low compared to mechanical press extraction process (40 – 45%). Furthermore, the quality of the oil depends on the settling which aims to eliminate water from the oil to avoid its oxidation. The by-product (handmade press cake) from the handmade extraction is an oily brown paste with a high water content. In some instances, this by-product can be used to feed cattle (Charrouf and Guillaume, 2008; Moutik et al., 2021) or to produce soaps and shampoo by handcrafted lavenders (Charrouf and Guillaume, 2008). In most cases, it is discarded because it is considered as a waste which is unfortunate because it was shown that oil extracted from this by-product is highly valuable (Charrouf and Guillaume, 2008; Moutik et al., 2021; Rojas et al., 2005). Nowadays, the study of the

* Corresponding author.
E-mail address: adil.mouahid@univ-amu.fr (A. Mouahid).

Nomenclature

a_s	specific area between the regions of intact and broken cells (m^{-1}).
C_u	solute content in the untreated solid ($kg_{oil}/kg_{biomass}$).
d_p	mean particle diameter (m).
e	extraction yield of the mathematical model ($kg_{oil}/kg_{insoluble\ biomass}$).
E	amount extracted (kg).
k_s	solid-phase mass transfer coefficient ($m.s^{-1}$).
K	partition coefficient.
n	number of experimental points.
N	solid charge in the extractor (kg).
N_m	charge of insoluble solid (kg).
P	pressure (bar).
q	relative amount of the passed solvent ($kg_{CO2}/kg_{insoluble\ biomass}$).
q'	specific flow rate ($kg_{solvent}/kg_{solid}/s$).
$\dot{Q}$	solvent flow rate (kg/s).
r	grinding efficiency or fraction of broken cells.
T	temperature (K).
t	extraction time (s).
x_t	transition concentration ($kg_{oil}/kg_{insoluble\ solid}$).
x_u	concentration in the untreated solid ($kg_{oil}/kg_{insoluble\ biomass}$).
y_s	apparent solute solubility (kg_{oil}/kg_{CO2}).

Greek letters

γ	solvent to matrix ratio in the bed ($kg_{solvent}/kg_{insoluble\ solid}$).
ε	bed void fraction.

extraction of compounds of interest from by-products (agro-waste) is a subject of high interest (Dey et al., 2021).

To our knowledge, only five studies about the valorisation of argan press cake can be found in the literature (Benmassaoud et al., 2017; Moutik et al., 2021; Rahib et al., 2021; Taarji et al., 2018; Zeghlouli et al., 2021). The oil from the press cake was considered for feeding cattle (Moutik et al., 2021), dyeing applications (Benmassaoud et al., 2017), its emulsification properties (Taarji et al., 2018), and biofuels/bioenergy applications (Rahib et al., 2021; Zeghlouli et al., 2021). In these studies, no real alternative to the current use of the handmade argan press cake was proposed. It is worth noting that no studies about the valorization of residual oil from handmade press cake as edible oil were found in the literature despite its edible properties. As the handmade extraction process leads to a low yield compared to other extraction process, almost half of the edible oil remains in the cake, one can imagine the economical interest in recovering it using a green and efficient extraction method.

This study aims to investigate the ability of supercritical CO_2 (SC-CO_2) to extract edible oil from handmade argan press cake in order to enable Moroccan cooperatives to improve their economic situation by valuing the handmade argan press cake. The extraction efficiency of oil from argan kernels by SC-CO_2 was shown in previous studies (Mouahid et al., 2022, 2021) and its capability to valorise agro-waste can be found in these recent studies (Bardeau et al., 2015; Campalani et al., 2020; Sánchez-Camargo et al., 2019). SC-CO_2 extraction is a very good alternative to organic solvent extraction. Indeed, CO_2 is non-toxic, its solvent power and selectivity towards neutral lipids can be improved by tuning temperature and pressure. Moreover, no separation step is needed since CO_2 is gaseous at ambient conditions of pressure and temperature. Lastly, CO_2 is recycled at industrial scale enabling a green and compact process.

2. Materials and methods

2.1. *Raw material and chemicals*

Handmade Argan press cake was provided by Moroccan Agricultural cooperative Khiorate Biladina. The water content of the sample was calculated by measuring its mass before and after air flow oven drying (Memmert, Schwabach, Germany) at 378 K for 24 h. The initial sample mass introduced in the air flow drying was about 5 g. The water content of the raw biomass was estimated at about 25 wt%. Extraction experiments were performed on air flow dried (AFD) biomass (drying at 318 K for 24 h), freeze-dried (FD) biomass and raw biomass (with and without glass beads of 2 mm diameter). The water content of the dried biomasses was estimated at about 5.5 wt% for both drying modes. Dried samples were ground and sieved at a mean particle diameter of 750 µm prior to extraction. The extractions experiments on raw biomass were conducted to check the possibility of avoiding the drying process. Uniform shape (ball shape) and non-uniform shape of about 1 cm of raw biomass (Fig. 1) were prepared prior to extraction to check the possibility of avoiding the use of glass beads. CO_2 was provided by Air Liquide (France) with a purity of 99.7%.

2.2. *SC-CO_2 extraction*

SC-CO_2 extraction experiments were performed on a laboratory scale extractor (Fig. 2) supplied by Separex (Champigneulles, France), an extraction autoclave of 20 cm^3 was used for the study. The detailed configuration of the extractor was given in previous study (Mouahid et al., 2021).

For each experiment, the mass of dried biomass introduced in the extraction autoclave lies between 6 and 9 g. The mass of extracted oil was estimated relative to the mass losses of the sample in the extraction autoclave ((6) in Fig. 2). The extraction kinetics were reported for the dried biomass.

When the extraction was performed on raw biomass, the mass of wet biomass lies between 4 and 6 g. The extractions were performed up to a CO_2/biomass mass ratio of about 62 kg/kg. The mass of extracted oil was estimated by weighting the collector tube located at the end of the extraction line ((7) in Fig. 2). The mass loss of the sample in the extraction autoclave ((6) in Fig. 2) was also measured as it represents the mass of both oil and water extracted from the sample. Water was not collected in the collector tube ((6) in Fig. 2) as it is driven by the gaseous CO_2 flux at the exit of the extraction line.

The yield was calculated considering Eq. 1. When dried sample is introduced in the extraction autoclave, the amount extracted (E) corresponds to the mass loss of the extraction autoclave. In the case of raw biomass sample introduced in the extraction autoclave, E corresponds to the mass of the oil collected in the collector tube. For the raw biomass, when the

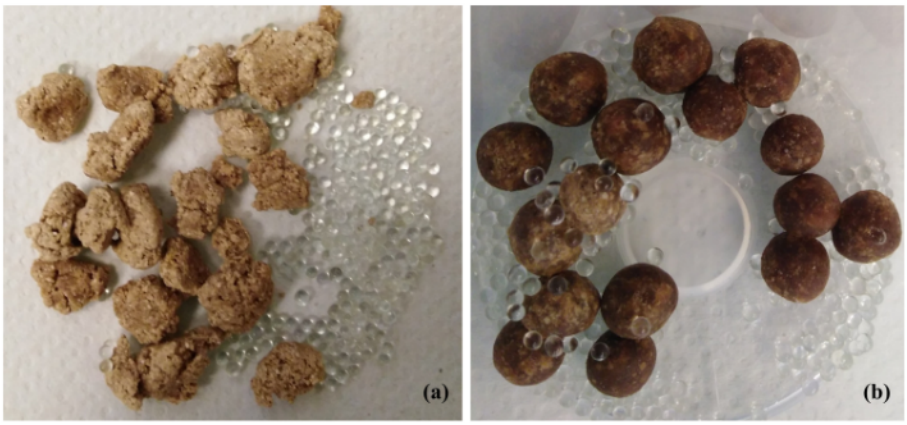

Fig. 1 – Pictures of prepared raw biomass with glass beads (a) non uniform shape after extraction experiment, (b) uniform shape after extraction experiment.

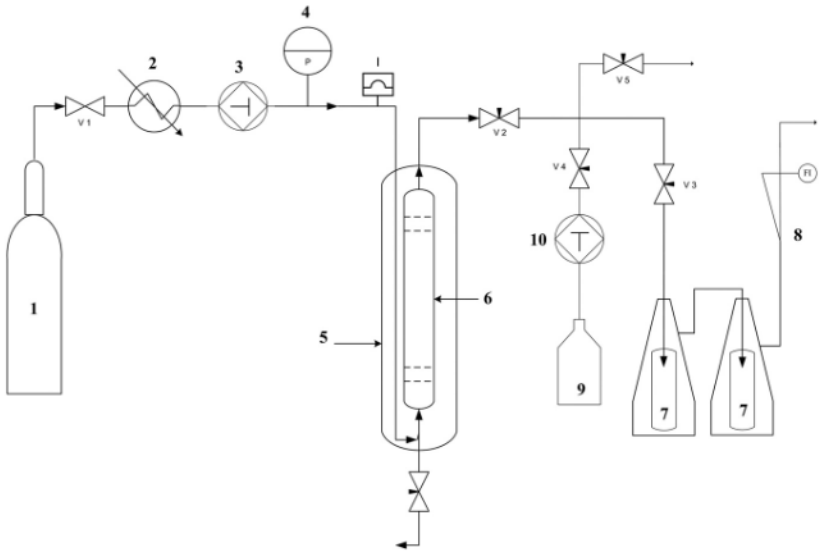

Fig. 2 – Process diagram of the extraction setup: (1) CO_2 tank, (2) cooler, (3) CO_2 high pressure liquid pump, (4) pressure gauge, (5) extraction apparatus heater, (6) extraction vessel, (7) oil collector glass vessel, (8) flowmeter, (9) ethanol tank, (10) Gilson high pressure solvent pump.

extraction of oil and water is considered, E represents the mass loss of the extraction autoclave.

$$Yield\,(kg/kg) = \frac{E\,(kg)}{mass\ of\ biomass\ introduced\ in\ the\ extractor\,(kg)} \quad (1)$$

The extraction curves were plotted as the variation of the yield as function of the CO_2/biomass mass ratio. Extraction experiments were conducted at 300 and 400 bar, 333 K at a SC-CO_2 flow rate of 0.14 kg/h. These operating conditions were chosen according to the results obtained in Mouahid et al. previous study on unroasted and roasted argan kernels (Mouahid et al., 2021).

2.3. Soxhlet extraction

For comparison, Soxhlet extractions, using *n*-hexane, were performed for 8 h, the mass sample was about 7.5 g. A volume of 125 mL of *n*-hexane was used for the extractions. The cycle duration was about 7 min. Hence, about 69 cycles were performed.

At the end of extraction, *n*-hexane was evaporated under vacuum in a rotary evaporator (Heidolph Laborota 4000) at 313 K. The extraction yield was estimated relative to the mass of extracted oil (Eq. 2).

$$\text{Soxhlet extraction yield}\,(kg/kg) = \frac{\text{mass of extracted oil}\,(kg)}{\text{biomass introduced in the Soxhlet apparatus}\,(kg)} \quad (2)$$

2.4. Extracted oil analysis

2.4.1. Fatty acid analysis

The extracted oils in isooctane were *trans*-methylated with a cold solution of KOH according to the European Standard NF EN ISO 5509 Norm (European Standard NF EN ISO 5509 Norm. (2000). Preparation of methyl esters of fatty acids. Paris, France: AFNOR) to obtain fatty acid methyl esters (FAME) which were analyzed by gas chromatography (Agilent gas chromatograph 7890 A, Agilent Technologies Inc., Santa

Clara, California) according to the European Standard NF EN ISO 5508 Norm (European Standard NF EN ISO 5508. (1995). Analysis by gas chromatography of methyl esters of fatty acids. Paris, France: AFNOR.). Hydrogen was used as a carrier gas with a flow of 1 mL/min. The instrument was equipped with a split/split-less injector (split ratio 1:60), a flame ionization detector and a Supelcowax 10 (Merck KGaA, Darmstadt, Germany) silica capillary column coated with polyethylene glycol (L×ID 60 m×0.25 mm, df 0.25 µm). The following temperature gradient was applied: 483 K during 20 min, then from 483 to 518 K at 6 K/min, and 518 K for 20 min. The data acquisition and processing were performed using Chemstation B.04.03-SPA (87) (Agilent) software.

2.4.2. *Tocopherol analysis*

Tocopherol analysis was carried out using an Agilent 1290 Infinity HPLC system equipped with a Quaternary Pump, an automatic liquid sample and a fluorimetric detector (FLD 1260). The detection was set at 295 nm for excitation wavelength and at 330 nm for emission wavelength. The separation column was a LiChrosorb® SI60 column (250 mm × 4.6 mm i.d., 5 µm, Merck KGaA Darmstadt, Germany). Elution was performed with HPLC grade solvents n-hexane/isopropanol (99/1, v/v) in isocratic mode at a flow rate of 1 mL/min, during 20 min. Column compartment was set at 298 K. Oil samples were dissolved in 1 mL of mobile phase before injection (1 µL). The identification of tocopherol isomers was confirmed by co-injection of a sample with authentic standards α-, β-, γ- and δ-tocopherols (Sigma Aldrich) then by comparison of retention time. Quantification of the 4 tocopherols was achieved according to the external standard method.

3. Modelling

The extraction curves were modelled using Sovová's BIC mathematical model (Sovová, 2005). As obtained in previous study on Argan kernels (Mouahid et al., 2022, 2021), the extraction type was found to be of type B. In the extraction of type B, the first part of the extraction curve is composed of two straight lines (Fig. 3) described by Eqs. 3 to 6. The first straight line (Eq. 3) is controlled by solute solubility in SC-CO_2. The second straight line (Eq. 5) indicates that the solute concentration in the biomass is considerably reduced, and the equilibrium is controlled by solute-matrix interactions. This implies that the solute concentration in the supercritical phase is much lower than its solubility. The transition between the two straight lines occurs at the transition concentration x_t: the solid-phase concentration becomes lower than "x_t" and all the solute interacts with the matrix. Hence, the transfer no longer depends on solubility but on the partition coefficient K which represents the constant of proportionality of the linear relationship between solid and fluid-phase concentrations. The transition concentration x_t is equal to the matrix capacity for interaction with the solute.

Solute-matrix interactions can be related to the desorption of the solute from the biomass. The last part of the extraction curve, described by Eq. 6, is controlled by solute diffusion from intact cells to broken cells.

- **First part of the extraction curve**

$$e = qy_s \text{ for } 0 \le q \le q_1 \tag{3}$$

with e, the extraction yield ($kg_{oil}/kg_{insoluble\ biomass}$)

$$q_1 = \frac{r(x_u - x_t) - \gamma K x_t}{y_s - K x_t} \tag{4}$$

$$e = q_1 y_s + (q - q_1) K x_t \text{ for } q_1 \le q \le q_c \tag{5}$$

- **Second part of the extraction curve**

$$e = x_u[1 - C_1 \exp(-C_2 q)] \text{ for } q > q_c \tag{6}$$

q_c is the value of q at the crossing point with the estimate for the second part of the extraction curve and.

- q_1 is the value of q at the crossing point with the first linear part and the second straight part considering the expression of q_1 in Eq. 4.

The second part of the extraction curve ($q > q_c$) is described by adjusting constant parameters C_1 and C_2. Estimations of parameters $k_s a_s$, the mass transfer coefficient, and r, the fraction of the broken cells, can be obtained by considering Eqs. 7 to 12:

$$r = 1 - C_1 \exp(-C_2 q_c) \tag{7}$$

$$k_s a_s = \frac{(1 - r)(1 - \varepsilon)\dot{Q} C_2}{N_m[1 - ((1 - r)C_2/K]} \text{ for } x_t > 0 \tag{8}$$

With:

$$e = \frac{E}{N_m} \tag{9}$$

$$q = \frac{\dot{Q}t}{N_m} \tag{10}$$

$$N_m = (1 - C_u)N \tag{11}$$

$$C_u = \frac{x_u}{1 + x_u} \tag{12}$$

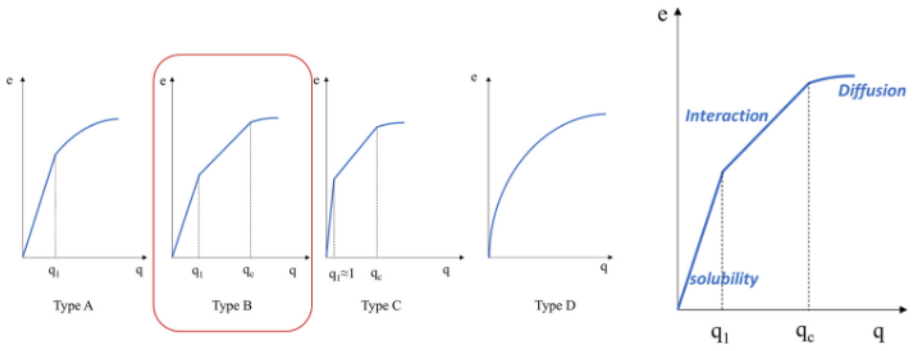

Fig. 3 – Extraction curve of type B according to Sovová's BIC model.

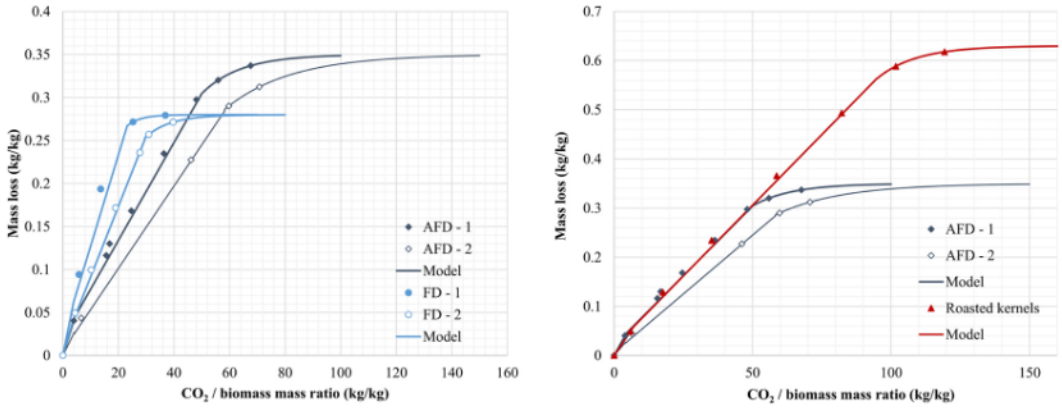

Fig. 4 – (a) Effects of drying mode on extraction kinetics and repeatability tests on AFD and FD biomass at 400 bar, 333 K and 0.14 kg/h, (b) Comparison between SC-CO_2 extraction kinetics obtained from AFD biomass and from roasted kernels at 400 bar, 333 K and 0.14 kg/h (d_p = 750 µm).

The adjustable parameters "C_1" and "C_2" were calculated by minimizing the sum of least squares between the experimental and calculated values of "e". The absolute average relative deviation (AARD) between the experimental and calculated yields, was used to evaluate the efficiency of the model.

4. Results and discussions

4.1. *Effects of drying mode and operating conditions on extraction kinetics*

The effects of drying and the effects of operating conditions are shown on Fig. 4 to Fig. 6. The experiments were performed on AFD and FD biomass at 300 and 400 bar, 333 K and 0.14 kg/h. The curves were modelled using Sovová's type B mathematical model, the model parameters are given in Table 1.

Regarding the repeatability tests (Fig. 4(a)) an average deviation ranging from 16% to 18% between the two sets of experiments was found for both AFD and FD biomass highlighting a poor repeatability. A non-uniform distribution of the oil in the Argan handmade press cake may explain these results. Indeed, the overall biomass is made up of a mixture of several handmade argan press cake coming from different harvests and from different workers. It is well-known that the quality of the manual work differs from a worker to another one leading to different extraction yields. It is then very difficult to obtain a good repeatability in the experiments. Nevertheless, a clear tendency was found regarding the extraction kinetics.

In Fig. 4(b), it can be observed that the extraction kinetic on roasted Argan kernel reported by Mouahid et al. (Mouahid et al., 2021) at the same operating conditions is very close to the extraction kinetics obtained on AFD biomasses. It is worth noting that the extraction kinetic AFD-1 is superimposed with the one obtained on roasted Argan kernels until the asymptotic yield was reached. This result may indicate that the surface structure of the AFD biomass is similar to the one of roasted kernels.

The drying mode (Fig. 4(a)) leads to very different results in terms of yield and extraction kinetics. Despite a high value of grinding efficiency parameter for both AFD and FD samples (r ≈ 90%) meaning a good efficiency of grinding and sieving, the highest extraction yield was found to be about 28% and about 35% for the FD and AFD biomass respectively. Similar yields were found after *n*-hexane extraction: about 28% and about 31% for the FD and the AFD biomass respectively. The highest yield, obtained on the AFD biomass, may be explained by the fact that after FD the biomass wall structures were less submitted to breakage (Crampon et al., 2013; Mouahid et al., 2016; Perrier et al., 2015) inducing a limitation of the SC-CO_2 diffusion. Indeed, the diffusion characterized by $k_s a_s$ parameter (Table 1) is lower when the extraction was performed on FD biomass at 400 bar and 333 K. Hence, the amount of accessible oil on the biomass depends on the applied drying mode.

The extraction kinetics obtained from FD biomass were found to be faster than the ones obtained from AFD biomass: the partition coefficient K of the FD biomass is two up to three times higher than the one obtained from the AFD biomass, and the value of q_c is about two times lower when the extraction was performed on the FD biomass. This result may be very surprising as in general, the freeze drying leads to slower extraction kinetics (Mouahid et al., 2016; Perrier et al., 2015). The drying mode should have caused very

Table 1 – BIC Model parameters for AFD and FD biomass.

Biomass	P (bar)	N (g)	y_s (g_{oil}/ $kgCO_2$)	C_1	C_2	$k_s a_s$ (s^{-1})	r	K	x_t (kg_{oil} / kg insoluble solid)	q_1 ($kg_{solvent}$ / kg_{solid})	q_c ($kg_{solvent}$ / kg_{solid})	γ (kg_{CO2} / $kg_{insoluble\ solid}$)	AARD (%)
AFD	300	7.959	7.914	1.290	0.020	4.273	0.70	9.510	0.500	4.473	48.326	1.147	3.04
AFD-1	400	8.956	10.371	4.478	0.046	3.157	0.87	11.473	0.495	4.232	49.817	1.235	4.14
AFD-2		5.313	6.629	2.123	0.027	4.523	0.82	9.249	0.517	4.068	58.250	1.235	3.07
FD-1	400	6.009	16.171	5.609	0.149	3.013	0.95	30.846	0.344	3.844	23.084	1.235	6.52
FD-2		7.998	11.314	2.535	0.080	2.878	0.90	22.722	0.360	3.636	29.528	1.235	2.91

different surface structures leading to very different behavior in the extraction kinetics.

The apparent oil solubility y_s was found to be higher when the extraction was performed on FD biomass, nevertheless as the distribution of the oil on the argan handmade press cake is not uniform it is difficult to confirm this tendency. The values of apparent oil solubility were found to be at the same order of magnitude than the one reported from roasted argan kernels at the same operating conditions (Mouahid et al., 2021).

The pictures of surface structures are shown in Fig. 5 for both biomasses before (Fig. 5(a) and (b)) and after extraction (Fig. 5(c) and (d)). Before extraction, for both biomasses, no porosity is visible probably due to the presence of a high amount of easily accessible oil at the surface of the particles. No clear difference between the two surface structures was identified in Fig. 5. This may be due to artifacts during SEM investigations, cryo-SEM may reveal the surface structures in more details to observe that FD biomass surfaces were less submitted to breakage. After SC-CO_2 extraction, the surface structures were found to be porous for both biomass which confirms the use of type B model. It is difficult to identify which biomass exhibit the highest porosity in Fig. 5(c) and (d). The fastest extraction kinetics obtained on FD biomass (Fig. 4) may be explained by differences in porosities between the FD biomass and the AFD biomass leading to less matrix-solute interactions.

One experiment was performed on AFD biomass at 300 bar and 333 K to study the effect of pressure variation on extraction kinetics. The results were reported in Fig. 6. The comparison with AFD-1 experiment (400 bar) showed that the partition coefficient K was found to be higher when the extraction was performed at 400 bar. The position of q_c is quite the same for both conditions (about 49 kg/kg), nevertheless the diffusion parameter $k_s a_s$ is slower at 300 bar. Consequently, the asymptotic extraction yield was reached at a higher CO_2/biomass mass ratio: about 150 kg/kg at 300 bar and about 90 kg/kg at 400 bar. The comparison with AFD-1 exhibits a faster extraction kinetic when the extraction was performed at 400 bar.

The comparison with AFD (300 bar) and AFD–2 experiment (400 bar) showed very similar values of the model parameters. Indeed, the values of K, $k_s a_s$ and y_s were found to be very close (deviation lower than 1%) leading to similar extraction kinetics. Nevertheless, the extraction kinetics at 400 bar is slightly faster than the one at 300 bar: the value of q_c is higher leading to an asymptotic extraction yield reached at a higher CO_2/biomass mass ratio of about 120 kg/kg.

In general, the extraction kinetics performed are faster at 400 bar. Nevertheless, due to the non-uniform distribution of oil on the biomass it remains unclear if the extraction kinetics at the higher pressure will cause significantly faster oil extractions. Considering these results and taking into

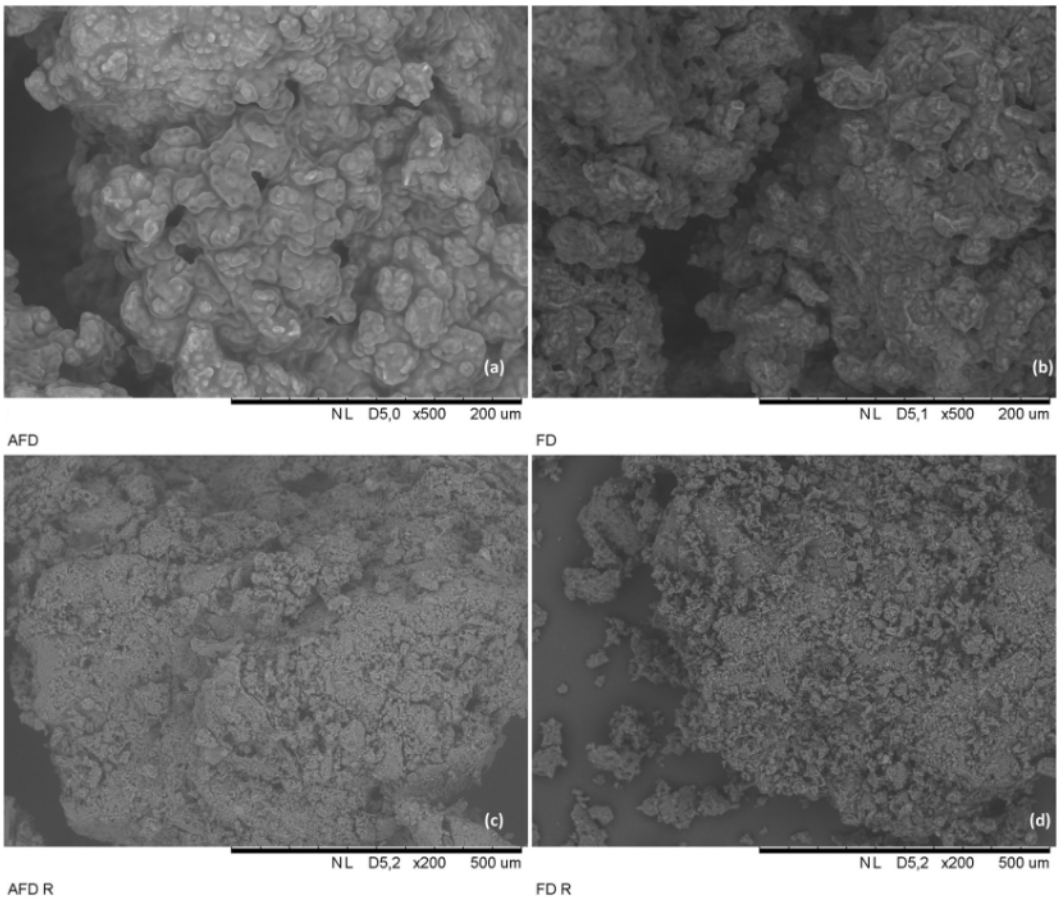

Fig. 5 – SEM images of (a) AFD biomass before extraction, (b) FD biomass before extraction, (c) AFD biomass after SC-CO_2 extraction at 400 bar - 333 K and (d) FD biomass after SC-CO_2 extraction at 400 bar - 333 K.

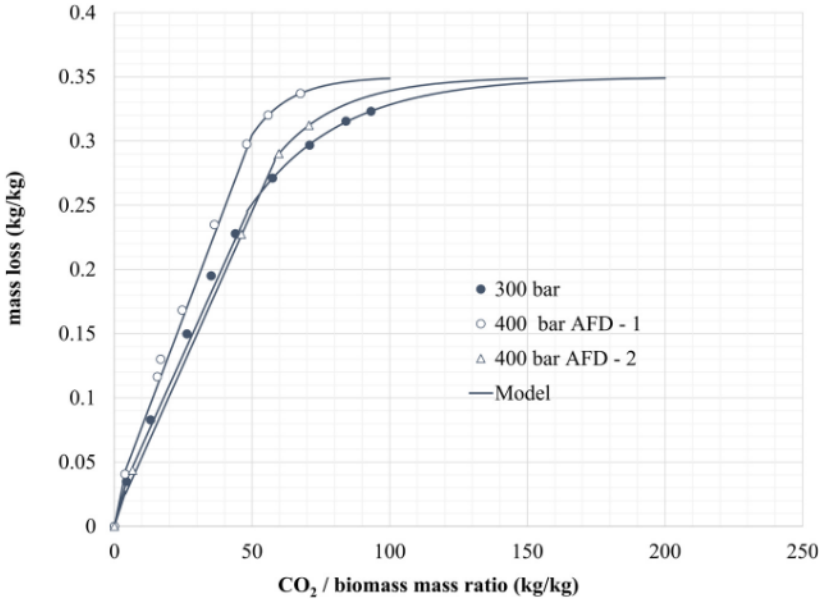

Fig. 6 – Effect of pressure on AFD biomass at 333 K and 0.14 kg/h.

account the operating costs, it may be more economically advantageous to work at a pressure of 300 bar.

4.2. SC-CO_2 extraction on raw biomass

SC-CO_2 extractions on raw biomass were performed at 300 bar, 333 K and 0.14 kg/h. The raw biomass was prepared as samples of uniform (ball shape) and non-uniform shape of about 1 cm size. The extractions were performed up to a CO_2/biomass mass ratio of about 62 kg/kg with or without glass beads of 2 mm diameter. The results were compared to AFD biomass extraction kinetics at 300 bar on Fig. 7.

The highest oil extraction yield, about 6.6%, was obtained on non-uniform shape with glass beads. The lowest extraction yield, about 1.1%, was obtained on ball shape biomass with glass beads. The extraction performed on ball shape without glass beads leads to an intermediary extraction yield of about 4.4%. For comparison, an extraction performed on ball shape biomass with glass beads at 400 bar, 333 K and 0.14 kg/h led to an oil yield of 2.72%. The yield of oil+water was found to be 7.15%. The increase of pressure didn't enhance the oil extraction yield. In this case, with the results obtained, it is difficult to conclude about the use of glass beads or the effect of the biomass shape (uniform or not) on the obtained extraction yield. Indeed, the variation in the SC-CO_2 extracted oil yield may be due to an irregular repartition of the glass beads in the extraction autoclave (size of glass beads lower than the size of the samples) and/or to the non-uniform distribution of oil and water in the homemade argan press cake. Indeed, the distribution of oil and water in each sample depends on the quality of the manual work of each worker. It is worth nothing that, in Moroccan cooperatives, after manual extraction the press cakes are mixed before being discarded.

The overall yield (water + oil) ranged from 7% to 23%, only the oil was collected in the collection tube. The water was driven by the flux of CO_2 at the end of the extraction line. This observation was reported in a previous study on *Nannochloropsis sp.* microalgae (Crampon et al., 2013). For this kind of biomass, the high-water content (about 25 wt%) acts

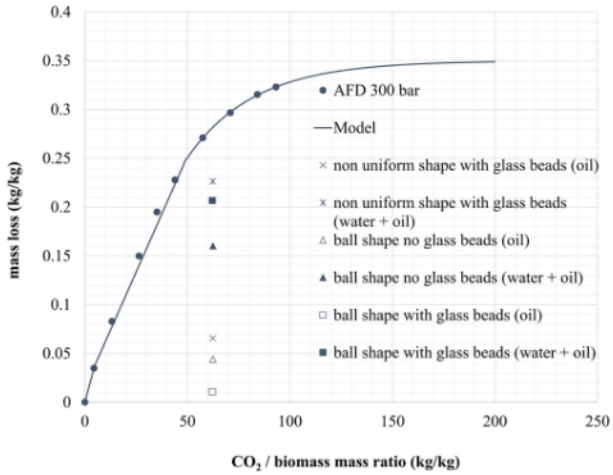

Fig. 7 – Extraction yield performed on raw biomass at 300 bar, 333 K and 0.14 kg/h.

Table 2 – FA composition in the oil extracted by SC-CO_2 and n-hexane from AFD, FD and raw biomasses.

Fatty acid		AFD (Soxhlet)	AFD (400 bar)	FD (400 bar)	Raw biomass (Soxhlet)	Rawbiomass (pellet – 300 bar)	Rawbiomass (non-uniform shape 300 bar)	Argapur*
Myristic acid	14:00	0.14	0.17	0.15	0.14	0.14	0.14	0.14
Palmitic acid	16:00	12.29	13.10	12.44	12.48	12.54	12.49	12.75
Stearic acid	18:00	5.43	5.00	5.43	5.47	5.51	5.35	5.7
Oleic acid	18:1ω9	45.72	45.21	45.54	46.58	46.43	46.53	46.26
Linoleic acid	18:2ω6	34.53	34.72	34.12	34.14	32.66	33.83	33.70
Arachidic acid	20:00	0.37	0.28	0.37	0.36	0.36	0.35	0.38
Gadoleïque acid	20:1ω9	0.36	0.29	0.37	0.37	0.35	0.34	0.34
Total identified		98.7	99.78	98.43	99.54	97.99	99.04	99.26

* Commercial edible oil

Table 3 – Tocopherols concentration in the oil extracted by SC-CO_2 from AFD, FD and raw biomasses.

Sample	Extraction method	α-tocopherol (mg/kg extract)	γ-tocopherol (mg/kg extract)	δ-tocopherol (mg/kg extract)	Total tocopherol (mg/kg extract)	Extracted mass (g)	Experimental oil extraction yield (%)
AFD Biomass	SC-CO_2 400 – 333 K	43.545	532.249	43.073	618.867	2.103	33.7
	Soxhlet	31.996	422.596	30.381	487.347	2.374	31
Raw biomass	SC-CO_2 300 – 333 K non uniform + glass beads	24.336	325.401	32.995	382.732	0.415	6.6
	SC-CO_2 300 – 333 K ball shape	0	12.427	14.534	26.96	0.372	4.4
	SC-CO_2 300 – 333 K ball shape + glass beads	0	0	0	0	0.053	1.1
	SC-CO_2 400 – 333 K ball shape + glass beads	0	39.167	21.64	60.931	0.124	2.72
	Soxhlet	6.952	102.043	25.246	135.178	0.937	12.5
Argapur	–	35.8	484.7	32.8	553.2	–	–

as a barrier to the diffusion of SC-CO_2 contrary to what was reported on *Dunaliella salina* microalgae (Mouahid et al., 2016) for which water acted as co-solvent.

4.3. *Extracted oils compositions*

Gas chromatography analysis of the fatty acid methyl ester of the oils extracted from AFD, FD and raw biomass by SC-CO_2 and n-hexane Soxhlet extractions are given in Table 2. The composition of the extracted oils was compared to a commercial edible oil (Argapur). The analysis showed that the fatty acids composition was similar for all samples. Indeed, whatever the sample and the pressure, the oils were mainly composed of palmitic (12.4 – 13.1%), stearic (5 – 5.4%), oleic (45.2 – 46.5%), and linoleic (32.6 – 34.7%) acids. The FA composition is similar to the one found for the commercial edible oil and the one found in previous studies for the SC-CO_2 extraction of unroasted and roasted Argan kernels (Mouahid et al., 2021).

Tocopherol analysis was performed on the oil extracted by n-hexane and SC-CO_2 from AFD and raw biomass. The results are reported in Table 3. The concentration of tocopherols in the oil extracted from AFD biomass by SC-CO_2 is at the same order of magnitude than the commercial edible oil suggesting that the oil recovered from the handmade argan press cake have a quality comparable to the commercial edible oil. It is worth noting that the composition corresponds to the recommendations of the official argan oil guidelines (Rahmani, 2005).

In the oil extracted by SC-CO_2 from raw biomass, the concentration of tocopherols was found to be very low. Indeed, the concentration of total tocopherols was found to be ranged from 2 up to 9 times lower than the one found for edible oil. Furthermore, for some experiments, no α-tocopherol was found in the extracted oil (Table 3). When the extraction was performed on ball shape biomass with glass beads at 300 bar, no tocopherols were detected. These variations in tocopherols concentration may be also due to different water content on each sample caused by the manual extraction method.

The high water content of the biomass may prevent an efficient extraction of tocopherols from the biomass.

When the oil was extracted by n-hexane from raw biomass, the concentration of total tocopherols was found to be about 2 times higher than the one obtained from SC-CO_2 except for the extraction performed on the non-uniform shape biomass. This difference may be due to the high number of cycles performed in the Soxhlet extractor leading first to the extraction of the water giving then access to the oil on the biomass. Indeed, the oil yield was found to be higher than the one obtained after SC-CO_2 extraction (12.5% for Soxhlet extraction and ranged from 1.1% to 6.6% for SC-CO_2 extraction).

5. Conclusion and perspectives

The SC-CO_2 extraction process was shown to be promising for the valorization of Argan handmade press cake. Indeed, the compositions of fatty acids and tocopherols extracted from dried biomass (which are similar to a commercial edible oil and to the oil extracted from roasted kernels (Mouahid et al., 2021)) correspond to the recommendations of the official argan oil guidelines.

The amount of accessible oil on the biomass ranged from 28% to 35% depending on the drying mode. A drying step is necessary to avoid the presence of high water content which acts as a barrier for SC-CO_2 diffusion and to avoid the oil oxidation. The SC-CO_2 extracted oil from dried biomass is a high oil quality comparable to the commercial edible oil considering the fatty acids and total tocopherols. To confirm these results, as the presence of water is known to promote oil oxidation, a perspective work would be the study of the effects of storage times on the biomass (which may have caused different levels of fat oxidation) and perform oxidation analysis as peroxide value to evaluate the oxidative deterioration of the extracted Argan oil.

AFD may be the most adequate drying mode as it leads to a higher extraction yield, despite a lower extraction kinetic. Furthermore, since it is well-known that the sunshine level in south of Morocco is strong, the AFD performed using solar energy may then be considered to lower the operation costs. With a similar strategy of reducing operating cost, the SC-CO_2 extraction can be considered at 300 bar instead of 400 bar.

The repeatability of the extraction kinetics was found to be poor due to a non-uniform distribution of oil on the handmade Argan press cake. Nevertheless, the extraction curves exhibit a clear tendency, and an interesting compromise may be found between a high yield (32%) and a lower CO_2/biomass mass ratio (100 kg/kg).

Author Contribution

The manuscript was written through contributions of all authors. All authors have given approval to the final version of the manuscript. These authors contributed equally.

Declaration of Competing Interest

The authors declare that they have no known competing financial interests or personal relationships that could have appeared to influence the work reported in this paper.

References

Bardeau, T., Savoire, R., Cansell, M., Subra-Paternault, P., 2015. Recovery of oils from press cakes by CO $_2$ -based technology. OCL 22, D403. https://doi.org/10.1051/ocl/2015004

Benmassaoud, Y., Villaseñor, M.J., Salghi, R., Jodeh, S., Algarra, M., Zougagh, M., Ríos, Á., 2017. Magnetic/non-magnetic argan press cake nanocellulose for the selective extraction of sudan dyes in food samples prior to the determination by capillary liquid chromatograpy. Talanta 166, 63–69. https://doi.org/10.1016/j.talanta.2017.01.041

Campalani, C., Chioggia, F., Amadio, E., Gallo, M., Rizzolio, F., Selva, M., Perosa, A., 2020. Supercritical CO_2 extraction of natural antibacterials from low value weeds and agro-waste. J. CO_2 Util. 40, 101198. https://doi.org/10.1016/j.jcou.2020.101198

Charrouf, Z., Guillaume, D., 2008. Argan oil, functional food, and the sustainable development of the argan forest. 1934578X0800300. Nat. Prod. Commun. 3. https://doi.org/10.1177/1934578X0800300237

Crampon, C., Mouahid, A., Toudji, S.-A.A., Lépine, O., Badens, E., 2013. Influence of pretreatment on supercritical CO_2 extraction from Nannochloropsis oculata. J. Supercrit. Fluids 79, 337–344. https://doi.org/10.1016/j.supflu.2012.12.022

Dey, T., Bhattacharjee, T., Nag, P., Ritika, Ghati, A., Kuila, A., 2021. Valorization of agro-waste into value added products for sustainable development. Bioresour. Technol. Rep. 16, 100834. https://doi.org/10.1016/j.biteb.2021.100834

Mouahid, A., Bombarda, I., Claeys-Bruno, M., Amat, S., Myotte, E., Nisteron, J.-P., Crampon, C., Badens, E., 2021. Supercritical CO_2 extraction of Moroccan argan (Argania spinosa L.) oil: Extraction kinetics and solubility determination. J. CO_2 Util. 46, 101458. https://doi.org/10.1016/j.jcou.2021.101458

Mouahid, A., Claeys-Bruno, M., Bombarda, I., Amat, S., Ciavarella, A., Myotte, E., Nisteron, J.-P., Crampon, C., Badens, E., 2022. Supercritical CO_2 extraction of oil from Moroccan unroasted Argan Kernels: Effects of process parameters to produce cosmetic oil. J. CO_2 Util. 59, 101952. https://doi.org/10.1016/j.jcou.2022.101952

Mouahid, A., Crampon, C., Toudji, S.-A.A., Badens, E., 2016. Effects of high water content and drying pre-treatment on supercritical CO_2 extraction from Dunaliella salina microalgae: Experiments and modelling. J. Supercrit. Fluids 116, 271–280. https://doi.org/10.1016/j.supflu.2016.06.007

Moutik, S., Benali, A., Bendaou, M., Maadoudi, E.H., Kabbour, M.R., El Housni, A., Es-Safi, N.E., 2021. The effect of using diet supplementation based on argane (Argania spinosa) on fattening performance, carcass characteristics and fatty acid composition of lambs. Heliyon 7, e05942. https://doi.org/10.1016/j.heliyon.2021.e05942

Perrier, B., Crampon, C., Guézet, O., Simon, C., Maire, F., Lépine, O., Pruvost, J., Lozano, P., Bernard, O., Badens, E., 2015. Production of a methyl ester from the microalgae Nannochloropsis grown in raceways on the French west coast. Fuel 153, 640–649. https://doi.org/10.1016/j.fuel.2015.03.011

Rahib, Y., Sarh, B., Chaoufi, J., Bonnamy, S., Elorf, A., 2021. Physicochemical and thermal analysis of argan fruit residues (AFRs) as a new local biomass for bioenergy production. J. Therm. Anal. Calor. 145, 2405–2416. https://doi.org/10.1007/s10973-020-09804-7

Rahmani, M., 2005. Composition chimique de l'huile d'argane " vierge ". Cah. Agric. 14, 461–465.

Rojas, L.B., Quideau, S., Pardon, P., Charrouf, Z., 2005. Colorimetric evaluation of phenolic content and GC-MS characterization of phenolic composition of alimentary and cosmetic argan oil and press cake. J. Agric. Food Chem. 53, 9122–9127. https://doi.org/10.1021/jf051082j

Sánchez-Camargo, A., del, P., Gutiérrez, L.-F., Vargas, S.M., Martinez-Correa, H.A., Parada-Alfonso, F., Narváez-Cuenca, C.-E., 2019. Valorisation of mango peel: Proximate composition, supercritical fluid extraction of carotenoids, and application as an antioxidant additive for an edible oil. J. Supercrit. Fluids 152, 104574. https://doi.org/10.1016/j.supflu.2019.104574

Sovová, H., 2005. Mathematical model for supercritical fluid extraction of natural products and extraction curve evaluation. J. Supercrit. Fluids 33, 35–52. https://doi.org/10.1016/j.supflu.2004.03.005

Taarji, N., Rabelo da Silva, C.A., Khalid, N., Gadhi, C., Hafidi, A., Kobayashi, I., Neves, M.A., Isoda, H., Nakajima, M., 2018. Formulation and stabilization of oil-in-water nanoemulsions using a saponins-rich extract from argan oil press-cake. Food Chem. 246, 457–463. https://doi.org/10.1016/j.foodchem.2017.12.008

Zeghlouli, J., Guendouz, A., Duchez, D., El Modafar, C., Michaud, P., Delattre, C., 2021. Valorization of co-products generated by argan oil extraction process: application to biodiesel production. Biofuels 1–7. https://doi.org/10.1080/17597269.2021.1941573